

Threading the Needle - Overtaking Framework for Multi-Agent Autonomous Racing

Suresh Babu, Varundev and Behl, Madhur

1 Abstract

2 Multi-agent autonomous racing still remains a largely
3 unsolved research challenge. The high-speed and close
4 proximity situations that arise in multi-agent autonomous
5 racing present an ideal condition to design algorithms which
6 trade off aggressive overtaking maneuvers and minimize the
7 risk of collision with the opponent. In this paper we study a
8 two vehicle autonomous racing setup and present AutoPass
9 - a novel framework for overtaking in a multi-agent setting.
10 AutoPass uses the structure of an automaton to break down
11 the complex task of overtaking into sub-maneuvers that
12 balance overtaking likelihood and risk with safety of the ego
13 vehicle. We present real world implementation of 1/10 scale
14 autonomous racing cars to demonstrate the effectiveness of
15 AutoPass for the overtaking task. **Our results indicate that**
16 **the overtaking success ratio for the AutoPass framework is**
17 **0.395 or 23 times more likely, compared to a purely**
18 **reactive system at 0.017, while traditional ROS based path**
19 **planners (depending on the navigation plugin used) are**
20 **placed between 0.115 to 0.286.**

21 Introduction

22 Demonstrating high-speed autonomous racing can be
23 considered a grand challenge for multi-agent robotics, and
24 for autonomous vehicles, and making progress in this arena
25 has the potential to enable breakthroughs in agile and safe
26 autonomy. To succeed at autonomous racing, an
27 autonomous vehicle is required to perform both precise
28 steering and throttle maneuvers in a physically-complex,
29 uncertain environment, and by executing a series of
30 high-frequency decisions. Autonomous racing is also
31 slowly becoming a motorsport featuring head-to-head battle
32 of algorithms. Roborace [1] is the Formula E's sister series,
33 which will feature fully autonomous race cars in the near
34 future. Autonomous racing competitions, such as F1/10
35 racing [2, 3], Autonomous Formula SAE, and Indy

36 Autonomous Challenge are, both figuratively and literally,
37 getting a lot of traction and becoming proving grounds for
38 testing perception, planning, and control algorithms at high
39 speeds and at the limits of controls.

40 Most past research in autonomous racing has focused on a
41 single-agent time-trial style of racing, i.e, a single
42 autonomous racecar completes a lap in the shortest amount of
43 time. Time-trial poses a number of challenges in terms of
44 dynamic modeling, on-board perception, localization and
45 mapping, trajectory generation and optimal control. Much
46 less attention has been devoted to the multi-agent style of
47 racing that we address in this paper. In addition to the
48 aforementioned challenges, multi-agent autonomous racing
49 also requires inferring the states of other agents, and
50 opportunistic passing while avoiding collisions. Multi-agent
51 autonomous racing provides the opportunity for testing
52 ground for developing and testing more widely applicable
53 non-cooperative multi-robot planning strategies.

54 In this paper, we examine a two-agent autonomous racing
55 setup to develop effective strategies for overtaking involving
56 autonomous agents that know each other's goals and
57 constraints. The contributions of the paper are:

- 58 1. We present AutoPass - an automaton-based framework
59 for high-speed overtaking in a multi-agent
60 autonomous racing setting. The AutoPass framework
61 distills the overtaking maneuver into canonical
62 sub-maneuvers such as approach, overtaking trajectory
63 synthesis, passing, and merge in front of the opponent.
- 64 2. We present an energy management system model that
65 accounts for boost energy depletion and recovery
66 during the race - a feature common in many
67 motorsports [4].
- 68 3. We demonstrate the effectiveness of our approach and
69 its ability to overtake safely on real F1/10 (one-tenth

70 scale) autonomous racing testbed [2] as well as on the
 71 ROS F1/10 autonomous racing simulator [3].

72 Our control architecture is modular and can fit into the
 73 perception, planning, and control stack of any autonomous
 74 racecar.

75 This paper is organized as follows: In Section 2, we present
 76 a detailed review of existing literature relevant to the
 77 problem of multi-agent autonomous racing. We then
 78 provide an overview of the Boost Energy system model in
 79 Section 3. The overtaking problem formulation is described
 80 in detail in Section 4, followed by the description of our
 81 novel AutoPass framework in Section 5. In Section 6, we
 82 evaluate the effectiveness of our proposed AutoPass
 83 framework in terms of successful overtakes for both
 84 simulated and real F1/10 autonomous racing testbed.
 85 Finally, we conclude the paper with a summary of the
 86 results and a brief discussion on future work in the
 87 conclusion Section 7.

88 Related Work

89 **Autonomous Overtaking:** Research on
 90 overtaking has focused mostly on free
 91 where the ego vehicle is tasked with s
 92 to pass a slower car. There have been
 93 on the best way to make this happen. A
 94 a method for overtaking a car using a
 95 with an emphasis on passenger comfort.
 96 in [8] demonstrates classical path planning
 97 for autonomous overtaking. These methods
 98 tested for structured autonomous driving
 99 and well-defined passing behaviors, as
 100 in autonomous racing. Authors in [9] de
 101 velop an overtaking strategy from a non-linear
 102 controller, while works demonstrated
 103 data-driven approaches to solving aut
 104 a simulated environment.

105 **Autonomous Racing:** The work done
 106 in [10] uses a game approach to autonomous racing,
 107 graph based trajectory planning for high
 108 speed racing, but it has several
 109 limits of control. An example of data
 110 high-speed autonomous racing is demon
 111 strated in [11] which is a high-speed
 112 overtaking framework, however, we fo
 113 described in [15] demonstrates how pi
 114 used for high-speed autonomous racing, but it has several
 115 drawbacks, such as corner-cutting, which can lead to
 116 collisions with the racetrack boundary. The authors in [16]
 117 propose using a model predictive controller for a high-speed
 118 racing controller that overcomes the corner-cutting problem,
 119 but this requires significant off-board computation and is
 120 compute and memory intensive. The work shown in [17]
 121 demonstrates an online implementation of MPC in an
 122 embedded robotic control system that is both fast and
 123 reliable for high speed autonomous racing. However, these
 124 methods are not capable of autonomous overtaking, except
 for [16] which can track and avoid dynamic obstacles, but

125 only in a reactive manner.

126 **Boost Energy Recovery and Management:** Boost energy
 127 is used in real motorsport racing as an aid in overtaking.
 128 Examples include the Formula 1 Kinetic Energy Recovery
 129 Systems [18] and Motor Generator Units [4], and the
 130 Indycar's Push-to-Pass system [19]. There is no related
 131 work in incorporating boost energy systems within
 132 autonomous racing overtaking approaches. This paper is
 133 among the first to address this problem.

134 Consequentially, in this paper we attempt to address
 135 shortcomings of these related efforts by presenting a new
 136 framework that uses a high-speed MPC controller that is
 137 capable of autonomous overtaking using the F1/10 racecar
 138 testbed and also by incorporating a boost energy
 139 management system capable of both recovering and using
 140 the stored boost energy. The framework is implemented
 141 using an automaton that lends itself well to model checking
 142 and design by verification methods in the future; such
 143 verification is not included in the current work.

144 Energy Management System

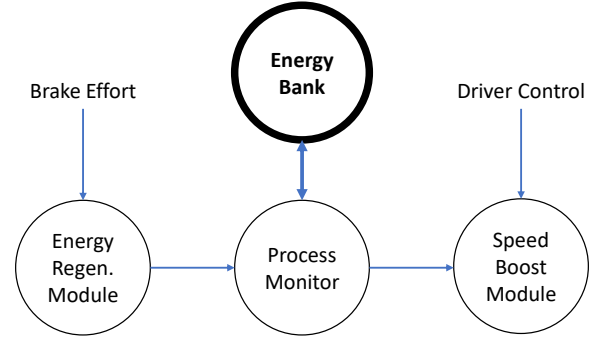


Figure 1: High level architecture of the Energy Management System (EMS).

145 In motorsport racing, overtaking involves using additional
 146 energy (boost) to move past an opponent. Racecars are
 147 fitted with dedicated boost energy control systems like the

Variable	Description	Value
Time step	q	0.1sec
Energy Bank	T	
Speed drain rate	ΔU	1% of T for 1q
Max. speed	u_{max}	
Speed boost	u_{boost}	25% of u_{max}
Brake effort	b	0A - 45A
Regeneration range	B	5A - 60A
Regen. capture rate	ΔT	0.1 for 1q

Table 1: The EMS control variables, with values during experiment. Demand values are between 0 and the stated max; drain rates indicated percentage from T for every q ; A is current amperage; v_{max} is continuous max speed.

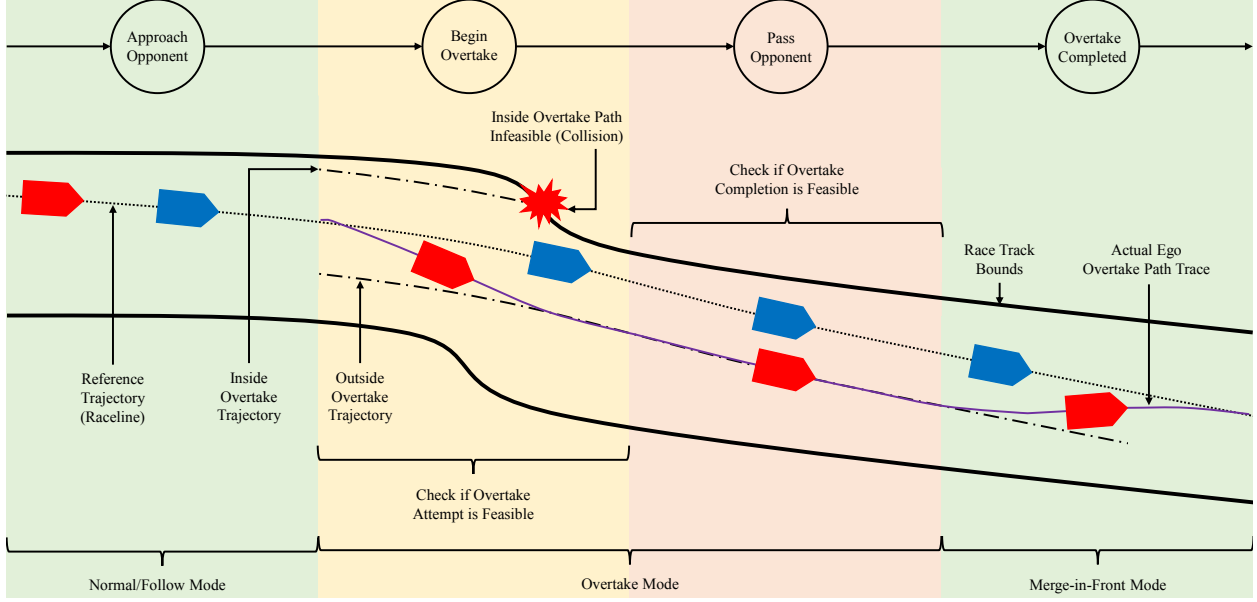


Figure 2: Overtake Stages for a Two Racecar Setup: the ego racecar (a) approaches the leading opponent, (b) chooses a feasible overtaking trajectory, (c) passes the opponent, and (d) safely merges in front of the opponent

148 F1 Motor Generator Unit (MGU) [4] and the Indycar’s
 149 Push-to-Pass system [19]. In some of the top motorsports,
 150 this boost energy has to be recovered by the racecar [4, 18]
 151 from its kinetic energy. In a similar manner, we created the
 152 Energy Management System (EMS) for our F1/10 [2]
 153 testbed to recover kinetic energy and provide boost energy
 154 to the racecar. The F1/10 testbed used in this paper has an
 155 electric drivetrain fitted with a motor controller
 156 (VESC [20]) capable of recovering, metering, and storing
 157 kinetic energy through regenerative braking. We created a
 158 virtual boost control system that allowed the F1/10 racecar
 159 to travel at a higher-than-maximum rated speed using the
 160 recovered energy for a fixed duration of time. The various
 161 parts of the EMS are shown in Figure 1. Energy recovery
 162 works by using the back-EMF from the axles to the motor,
 163 which is metered and stored in the main traction battery as a
 164 virtually separate entity (Energy Bank). When energy boost
 165 is necessary, the AEMS provides a dynamically controllable
 166 speed boost by drawing more power (peak power),
 167 which is subtracted from the Energy Bank. Normally the
 168 drivetrain is operated under continuous maximum power.

$$T_q = T_{q-1} + \Delta T; b \in B \quad (1)$$

$$v_q = v_{q-1} + u_{boost}; T_q = T_{q-1} - \Delta U$$

169 The energy regeneration and utilization are governed by the
 170 Equation 1 and Table 1 provides a list of variables used by
 171 the AEMS. The variable T_q models regenerative braking,
 172 while v_q models the dynamic boost energy utilized with
 173 proportional energy drain from the EMS.

174 Problem Formulation

175 Consider an ego racecar following a global raceline lagging
 176 an opponent racecar within its horizon. The objective for
 177 the ego racecar is to safely pass the leading opponent. The
 178 ego racecar approaches the opponent and generates a
 179 feasible overtaking trajectory to pass the opponent; the ego
 180 racecar estimates its chance of a successful overtaking and, if
 181 feasible, executes the overtaking maneuver in the sequence
 182 shown in Figure 2, while utilizing the available boost
 183 energy for overtaking as needed. A summary of the four
 184 stages of an overtaking maneuver is as follows:

- 185 • Approach Opponent: The ego racecar approaches the
 186 leading opponent and generates multiple overtaking
 187 trajectories to pass the opponent; the ego racecar
 188 estimates its chance of a successful overtaking.
- 189 • Begin Overtake: The ego racecar chooses a valid
 190 overtaking trajectory (if one exists) and verifies whether
 191 it has enough boost energy to pass the opponent, if so,
 192 it starts the overtaking maneuver.
- 193 • Pass Opponent: The ego racecar passes the opponent
 194 and takes the lead while continuing to estimate if the
 195 overtaking maneuver remains feasible on the current
 196 overtaking trajectory.
- 197 • Complete Overtake: The ego racecar clears enough
 198 distance in front of the opponent and attempts to take
 199 the lead position on the global raceline trajectory to
 200 continue the race. Otherwise the ego racecar abandons
 201 the overtaking.

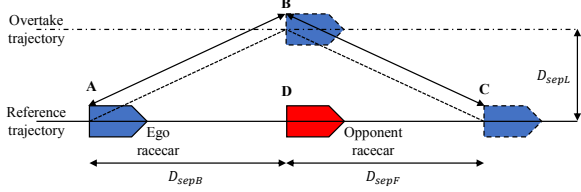


Figure 3: Approximated overtake geometry

202 Figure 3 provides an approximate geometry of this overtake
 203 maneuver. For the purpose of simplification, the ego racecar
 204 must not violate (a) the minimum rear separation distance
 205 D_{sepB} and minimum frontal separation distance from the
 206 opponent (D_{sepF}), and (b) the minimum separation from the
 207 fender of the opponent during overtake (D_{sepL}). The
 208 ego racecar must take the approximate path ABC (x_{tot})
 209 around the opponent, with the point B being on an overtake
 210 trajectory. Table 2 provides a brief description of notations
 211 used in this paper.

Notation	Description
x_{tot}	Total overtake path length
D_{sepL}	Lateral separation between racecars
D_{sepF}	Minimum front separation between racecars
D_{sepB}	Minimum rear separation between racecars
D_{Fmin}	Minimum follow distance
D_{Fmax}	Maximum follow distance

Table 2: List of notations used in AutoPass

212 The objective of the ego racecar is to safely pass the leading
 213 opponent. Assume the ego racecar is travelling at velocity
 214 (u_{ego}) and the opponent at (u_{opp}) with a differential
 215 velocity of the ego w.r.t. the opponent at (δu). The ego
 216 racecar must travel along the path ABC (see Figure 3),
 217 which is the total overtake path length (x_{tot}) calculated
 218 using Equation 2. Here, we assume D_{sepB} and D_{sepF} are
 219 the same. Additionally, in the right triangle ABD from
 220 Figure 3, AB is the hypotenuse, BD is the height which is
 221 D_{sepL} and the base AD is the sum of the initial vehicular
 222 separation (D_{sepB}) and the differential progress made by
 223 the opponent while the ego travels along the hypotenuse
 224 until it reaches the apex at B. We calculate the hypotenuse
 225 BC of the right triangle BDC in the similar method. Since
 226 D_{sepB} and D_{sepF} are similar, the right triangles ABD and
 227 BDC are the same as long as the opponent's velocity does
 228 not change during the overtake maneuver, thus the total
 229 overtake path (x_{tot}) is the sum of the hypotenuse AB and
 230 AC. Equation 2 explains this mathematically. Equation 2 is

231 formulated in the moving frame of the opponent.

$$\begin{aligned}
 \delta u &= u_{ego} - u_{opp} \\
 AB &= (AD^2 + BD^2)^{1/2} \\
 &= ((D_{sepB} + \delta u * t)^2 + D_{sepL}^2)^{1/2} \\
 BC &= (DC^2 + AD^2)^{1/2} \\
 &= ((D_{sepF} + \delta u * t)^2 + D_{sepL}^2)^{1/2} \\
 x_{tot} &= AB + BC \\
 &= 2 * ((D_{sepB} + \delta u * t)^2 + D_{sepL}^2)^{1/2}
 \end{aligned} \tag{2}$$

232

233 From Equation 2, ($\delta u * t$) is the differential progress made
 234 by the ego racecar w.r.t. to the opponent during the time
 235 period t . A positive (δu) is necessary for a successful
 236 overtake i.e., the velocity of the ego racecar greater than the
 237 velocity of the opponent. It is also assumed that both the
 238 ego racecar and the opponent have non-zero velocities.

239 The problem is to find an efficient and feasible way to use
 240 the boost energy during the overtake maneuver such that the
 241 likelihood of the completion of the maneuver can be
 242 computed ahead of time. For this, we compute the
 243 minimum value for $u_{ego} + u_{boost}$ (boosted speed) that
 244 would satisfy Equation 3. The boosted speed is the sum of
 245 the normal speed of the racecar and the temporary increase
 246 over the maximum continuous speed provided by the energy
 247 management system (EMS). The boosted speed
 248 ($u_{ego} + u_{boost}$) is capped at ($u_{max} + u_{boost}$). The energy
 249 management system in section 3 and Table 1 provides more
 250 information about these variables and how they are
 251 controlled by the AutoPass framework.

$$t = 2 * \sqrt{\frac{D_{sepL}^2}{(u_{ego} + u_{boost})^2 - u_{opp}^2}} \tag{3}$$

252 The value t is the boost energy budget (in terms of time)
 253 assigned to the overtake maneuver from the Energy Bank
 254 (T). This means that the ego racecar has the time target t to
 255 reach the end of the overtake path. Figures 2 and 3 along
 256 with Table 1 provide more information about the variables.

257 We have made the following assumptions in this paper: (a)
 258 the ego racecar is only tasked with overtaking an opponent
 259 and is not expected to defend its position if the opponent
 260 initiates an overtake, (b) the ego racecar is capable of
 261 accurately estimating the vehicle state of the opponent (incl.
 262 position, velocity, etc.), (c) the ego racecar is aware of the
 263 opponent's racing strategy, and (d) we currently assume a
 264 two racecar setup i.e., one ego and one opponent racecar.

265 AutoPass Framework

266 To fully implement the above sequence and to account for
 267 scenarios where an overtake may not be possible, current
 268 overtake becomes infeasible, or opponent attempts to block
 269 an overtake attempt, the ego racecar must continuously
 270 track the opponents state and accurately predict the
 271 opponent's future state. The entire framework's architecture
 272 is shown in Figure 4. The framework works simultaneously
 273 to (a) estimate ego and opponent states, (b) make decisions
 274 based on an overarching racing strategy, and (c) implement
 275 the chosen strategy on the ego racecar's race controller. The
 276 three modules are connected to an overtake state machine (a
 277 finite state automaton) to precisely execute the correct
 278 racing behaviour before, during, and after an overtake
 279 attempt. The state machine (AutoPass automaton) is
 280 described in detail in the next sections.

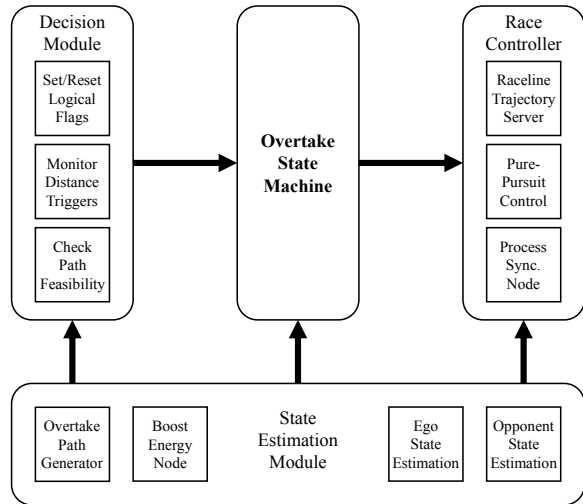


Figure 4: Overtake Control Architecture, showing the various functional modules and their interdependent relationships

281 **State Estimation Module** The observable states of the ego
 282 racecar and the opponent are estimated using a fast
 283 approximate particle filter [21]. These states include
 284 position in racetrack and absolute velocities, which helps
 285 extrapolating into the future to calculate future states as
 286 well. The ego racecar's internal state estimation includes
 287 the B.E.M. and the overtake path generation. In our setup,
 288 the ego racecar produces several parallel trajectories to the
 289 main raceline equally spaced using the largest dimension of
 290 the ego and the opponent base footprint. The overtake
 291 trajectories are generated by projecting the global raceline
 292 by a constant offset from the geometric center of the
 293 racetrack. The offsets used in this paper is a multiple of
 294 D_{sepL} . To judge the feasibility of the overtake paths, we
 295 checked for potential collisions with the racetrack bounds
 296 using a simple ROS occupancy grid search of the racetrack.

297 **Decision Module** The ego racecar must maintain safe
 298 distances from the opponent in addition to the constraints
 299 imposed by the navigation stack. These are a set of distance

300 triggers that help in calculating the logical inputs to the
 301 overtake state machine:

- 302 • D_{Fmin} - the minimum follow distance, which is the
 303 closest the ego racecar is allowed to follow the leading
 304 opponent without risking collision or violating the ego
 305 racecar's constraints.
- 306 • D_{Fmax} - the maximum follow distance, which is the
 307 farthest the ego racecar is allowed to follow the
 308 leading opponent when in the follow state (more info
 309 next section).
- 310 • D_{sepF} - the minimum frontal separation, which is the
 311 minimum distance the ego racecar must achieve
 312 between the front fender of the opponent and the rear
 313 fender of the ego during overtake to be allowed to
 314 merge in front of the opponent.
- 315 • D_{sepB} - the minimum rear separation, which is the
 316 absolute minimum distance between the front fender
 317 of the racecar and the rear fender of the opponent that
 318 the ego racecar must achieve to consider the current
 319 overtake abandoned.

320 **Race Controller** The ego racecar is controlled by a robust
 321 Ackermann-steering adjusted pure-pursuit path planner [22]
 322 and a global trajectory server using costmap and occupancy
 323 grid layers from the Robot Operating System (R.O.S.). The
 324 trajectory server breaks down the given trajectory whether it
 325 is the reference raceline or the chosen overtake trajectory
 326 path into a set of equidistant waypoints that the pure-pursuit
 327 controller can use to navigate around the race track at high
 328 speeds. For our current implementation, we chose
 329 pure-pursuit over more sophisticated controllers such as the
 330 Model Predictive Controller described in [23] because of
 331 the ease of hardware implementation and computational
 332 simplicity. The pure-pursuit controller used in this paper
 333 may not be well suited for a full-scale racecar [24, 25]. Our
 334 decision to use the pure-pursuit controller over more
 335 sophisticated model-based controllers shown in [24, 25], is
 336 because (a) our F1/10 testbed [2] is based on a scaled
 337 radio-controlled (RC) car, and (b) our test race-track short
 338 and wide enough to reasonably accommodate the path
 339 tracking error and limitations of the pure-pursuit planner
 340 used. We have made the AutoPass framework modular in
 341 order to accommodate different race controllers (see
 342 Figure 4) as long as the necessary state information is made
 343 available from the race controller to the rest of the AutoPass
 344 framework. As can be seen in Figure 4, the right hand side
 345 is the race controller which comprises the following nodes
 346 that (a) monitor the pose of the ego racecar on the global
 347 raceline, (b) provide the synchronization signal for the other
 348 nodes in the AutoPass framework, and (c) provide steering
 349 and throttle commands to the vehicle controller. The scope
 350 of our work is focused on designing the architecture and
 351 algorithm for the overtake maneuver - which itself is
 352 decoupled from the low-level controller i.e. a different race
 353 controller such as MPC could be used in place of
 354 pure-pursuit. The race controller provides the timing signal

355 necessary to synchronize all the processes in the AutoPass
 356 framework. The race controller also
 357 traction effort to overcome wheel-sli

358 We chose an automaton to implemen
 359 framework as it allowed us to easily
 360 assumptions about how the overtake
 361 structured, and in the future, we will
 362 model check our framework.

363 The overtake state machine is define
 364 $(\mathcal{P}, \mathcal{M}, \mathcal{I}, \delta)$, with P inputs, M stat
 365 and $\delta = P \times M$ is the set of transitio
 366 The state estimation module provide
 367 machine.

368 Figure 5 shows the AutoPass automa
 369 conditions governing state transition

370 **Inputs**

371 **Relative Path Progress (y_{gap})**

372 The distance y_{gap} is the absolute pat
 373 racecars. It is the product of differen
 374 of the corresponding racecar on the i
 375 resolution (actual distance between successive waypoints).
 376 We calculate the path distance instead of the minimum
 377 distance between racecars due to the geometric
 378 complexities of the racetrack.

$$y_{gap} = \arg \min(y_{ego} - w_i) - \arg \min(y_{opp} - w_i) \quad (4)$$

379 In Equation 4, w_i is a waypoint along the global raceline
 380 (or, reference trajectory) and the function $\arg \min$ is
 381 calculating the index of the waypoint closest to the racecar's
 382 *base_link* (geometric center of racecar control - usually at
 383 the center of the rear axle).

384 **Overtake Flag (OTF)** The overtake flag (OTF) is a
 385 boolean flag that checks if an overtake maneuver is feasible
 386 by comparing the resources requested for the overtake and
 387 the resources available to the race controller. It takes into
 388 account the feasibility of the list of overtake trajectories
 389 generated and chooses the best trajectory to execute the
 390 overtake using minimum amount of boost energy available.

391 **Position Match Flag (PMF)** This input is a boolean flag
 392 that is set when the relative path progress is zero for the first
 393 time during the attempted overtake maneuver to separate the
 394 trigger conditions between the overtake attempt and merge
 395 front maneuver.

396 **Safe Fall Back Flag (SFB)** When an overtake attempt
 397 fails, the ego racecar is designed to transition to the the
 398 follow mode behind the opponent racecar, and the safe
 399 fallback flag is a boolean flag that is set *True* when all

400 safety distance thresholds have been met.

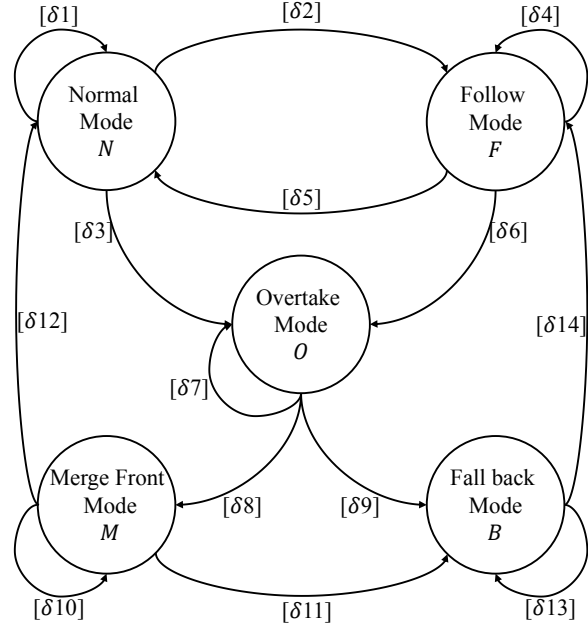


Figure 5: The AutoPass automaton, showing the different states involved in an overtake attempt and the transition (guard) conditions between the states

401 **States**

402 **Normal Mode** In this state, the ego racecar executes normal
 403 racing behavior on the raceline while within the same mode
 404 [δ1]. Two transitions are possible from this state to (a)
 405 Follow Mode and (b) Overtake Mode, as defined by guard
 406 conditions [δ2] and [δ3]

$$\begin{aligned} \delta 1 &: |y_{gap}| < D_{Fmin} \\ \delta 2 &: |y_{gap}| \in [D_{Fmin}, D_{Fmax}] \& \neg OTF \\ \delta 3 &: |y_{gap}| \in [D_{Fmin}, D_{Fmax}] \& OTF \end{aligned} \quad (5)$$

407 **Follow Mode** In follow mode, the ego racecar maintains a
 408 safe following distance from the opponent racecar while on
 409 the raceline [δ4] with two possible transitions to (a) Normal
 410 Mode and (b) Overtake Mode, as defined by guard
 411 conditions [δ5] and [δ6]

$$\begin{aligned} \delta 4 &: |y_{gap}| \in [D_{Fmin}, D_{Fmax}] \& \neg OTF \\ \delta 5 &: |y_{gap}| < D_{Fmin} \\ \delta 6 &: |y_{gap}| \in [D_{Fmin}, D_{Fmax}] \& OTF \end{aligned} \quad (6)$$

412 **Overtake Mode** In overtake mode, the racecar follows the
 413 selected overtake trajectory [δ7] while continuously

414 monitoring the progress of the overtake maneuver against
 415 the available controller resources with two possible
 416 transitions to (a) Merge Front Mode and (b) Fall Back
 417 Mode, as defined by the guard conditions $[\delta 8]$ and $[\delta 9]$

$$\begin{aligned} \delta 7 &: OTF \& !PMF \\ \delta 8 &: OTF \& PMF \\ \delta 9 &: !OTF \end{aligned} \quad (7)$$

418 **Merge Front Mode** In merge front mode, the ego racecar is
 419 tasked with merging back onto the main raceline in front of
 420 the opponent racecar $[\delta 10]$ while maintaining a safe
 421 distance from the opponent racecar with two possible
 422 transitions to (a) Normal Mode and (b) Fall back Mode, as
 423 defined by the guard conditions $[\delta 11]$ and $[\delta 12]$. The
 424 current design of the Merge Front mode assumes that the
 425 opponent is unable (incapable, too aggressive, etc.) to avoid
 426 a collision with the ego, thus forcing the ego to not violate
 427 its safety constraints and ultimately abandon an overtake.

$$\begin{aligned} \delta 10 &: |y_{gap}| \leq D_{sepF} \& OTF \& PMF \\ \delta 11 &: |y_{gap}| > D_{sepF} \\ \delta 12 &: !OTF \& !PMF \end{aligned} \quad (8)$$

428 **Fall Back Mode** If the current overtake attempt becomes
 429 infeasible, the ego racecar transitions to the Fallback state.
 430 In this state, the ego racecar engages its full available
 431 braking power to prevent a collision with the opponent or
 432 the racetrack bounds $[\delta 13]$. The primary objective of the
 433 fallback state is to prevent an impending collision and then
 434 safely guide the ego racecar back to the global raceline
 435 $[\delta 14]$ in the normal mode.

$$\begin{aligned} \delta 13 &: |y_{gap}| \leq D_{sepB} \& !SFB \\ \delta 14 &: |y_{gap}| > D_{sepB} \& SFB \end{aligned} \quad (9)$$

436 The AutoPass framework is currently designed only to
 437 overtake an opponent and cannot defend the ego racecar's
 438 position from an attempted overtake by an opponent. Each
 439 state's output enables the different behaviours that make up
 440 the various overtake sequences. More information about the
 441 overtake sequences are described in the experiments
 442 section.

443 Experiments & Results

444 **Experiment Setup** We chose the F1Tenth racecar [2]
 445 platform for our experiments and conducted multiple tests
 446 using an indoor racetrack. We deployed two autonomous
 447 F1Tenth racecars in real world and the racing simulator [3].

448 The opponent racecar was initialized in the lead position for
 449 all experiments, and each experiment was 25 laps long for
 450 different values of boost energy and opponent advantage,
 451 with a total of 225 laps across all different variables on the
 452 physical testbed and 600 laps in simulation leading to a total
 453 of 33 experiments covering all variables).

454 **The Ego Racecar** was deployed with the AutoPass
 455 framework, while the **Opponent Racecar** was made to
 456 autonomously navigate the racetrack on the global raceline
 457 at high speeds using a pure-pursuit controller. Each racecar
 458 used a single 2D planar scanning LiDAR as the primary
 459 perception and navigation sensor with a feedback enabled
 460 motor and steering controller providing odometry data.
 461 Both LiDAR and odometry data were used by an online
 462 GPU particle filter [21] for fast and dependable localization
 463 at high speeds around the racetrack. To simplify the ability
 464 of the ego racecar in tracking the opponent, we enabled
 465 *base_link* (which is the standard ROS name for the
 466 racecar's main control frame) sharing across both racecar's
 467 through a centralized control computer.

468 Figure 6 shows two outcomes of the AutoPass framework
 469 implemented on the F1Tenth racecars. The left half of the
 470 figure shows the ego racecar attempting to overtake the
 471 opponent from the outside of the turn and running out of
 472 boost energy, thus abandoning the overtake attempt. The
 473 right half of the figure shows the ego racecar attempting to
 474 pass the opponent from the inside of the turn using the boost
 475 energy provided to successfully pass the opponent and
 476 continue on the global raceline. This behavior in Figure 6 is
 477 similar to those observed in real motorsport racing.

478 **Defined Overtake Sequences** Figure 7[Left] provides the
 479 complete state transition sequence for the different overtaking
 480 sequence labels described in this section. Each of the
 481 sequence labels define the outcome of an overtaking attempt

- 482 • **High Speed Overtake:** (best case scenario), when the
 483 ego racecar approaches the opponent at a high speed,
 484 it immediately attempts an overtake because an
 485 overtaking trajectory exists and completes the overtaking
 486 by merging in front of the opponent. The ego racecar
 487 uses very little boost energy in this case.
- 488 • **Normal Overtake:** the ego racecar approaches the
 489 opponent and determines that an overtake is currently
 490 infeasible, so it follows the opponent until an overtaking
 491 attempt is feasible and executes the overtaking maneuver
 492 using the boost energy and successfully passes the
 493 opponent then merges in front of the opponent
- 494 • **Normal Abandoned Overtake:** the ego racecar
 495 executes the Normal Overtake sequence because it
 496 estimated that the overtaking was feasible but a
 497 recalculation with updated state information finds that
 498 the attempt is no longer feasible (eg: ego racecar uses
 499 the entire boost energy before the attempt is
 500 successful, the opponent manages to increase the
 501 lateral separation during the attempt etc.) forcing the

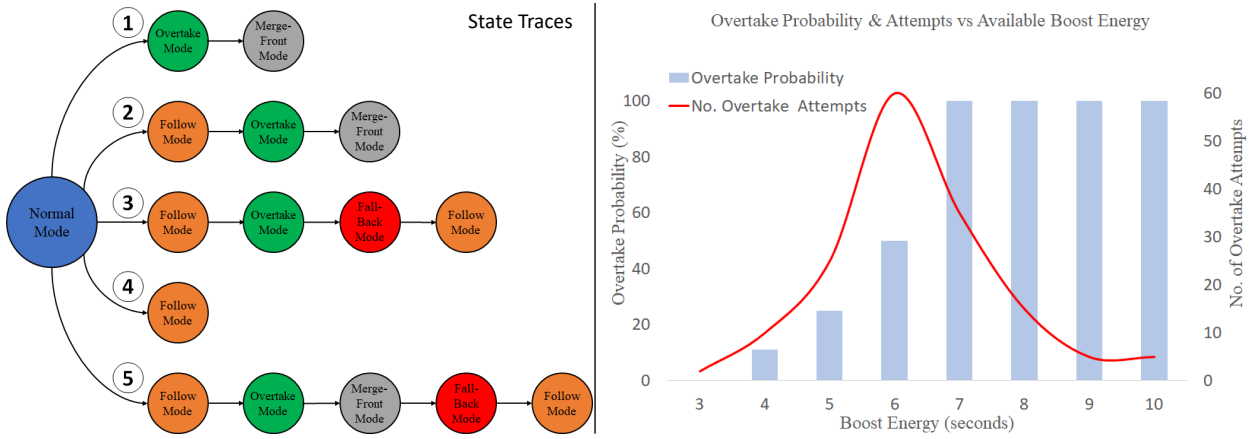


Figure 7: [Left]: Traces labels of valid state transitions (1) high speed overtake, (2) normal overtaking, (3) normal abandoned overtake, (4) overtaking infeasible, and (5) hybrid abandoned overtaking; [Right]: Overtake probability and attempts vs boost energy. Red trace is the overtaking probability and Blue histogram is the size of the boost energy bank T

502 ego racecar to fallback behind the opponent declaring
 503 the overtaking unsuccessful

504 • Overtake Infeasible: The ego racecar approaches the
 505 leading opponent but an overtaking attempt is infeasible
 506 and will continue to remain infeasible for an extended
 507 time (narrow racetrack, not enough boost energy etc.),
 508 thus making the ego racecar follow the opponent in
 509 perpetuity until an overtaking attempt becomes feasible

510 • Hybrid Abandoned Overtake: the ego racecar
 511 successfully passes the opponent in an overtaking
 512 attempt but estimates that a merge-front maneuver
 513 might violate safety constraints (e.g. when the
 514 opponent is overly aggressive and denies the ego an
 515 opportunity to complete the merge front maneuver by
 516 forcing an imminent collision between the racecars,
 517 etc.), thus the ego racecar abandons the current
 518 overtaking attempt using all available braking effort to
 519 safely fallback behind the opponent. This trace is not
 520 frequently observed, but it shows the robustness of the

521 AutoPass framework and its designed emphasis on
 522 vehicular safety

523 Figure 7[Right] shows (a) the probability that an overtaking
 524 attempt may be successful for an experiment for the different values
 525 of boost energy available, and (b) the number of overtaking
 526 attempts for the corresponding values of boost energy. The
 527 results from this figure show that the probability of a
 528 successful overtaking proportionally increases with the
 529 available boost energy. An interesting note here is that the
 530 ego racecar attempts to overtake the most number of times
 531 when the probability of success is around 50%, and
 532 continues to decrease with higher boost energy values
 533 showing that the ego racecar attempts fewer overtakes, but
 534 successfully completes each attempt at the higher boost
 535 energy values. This is because, in our two car experiment
 536 setup, when an overtaking attempt is guaranteed to be
 537 successful - and the racecar does successfully overtake an
 538 opponent, it returns to the Normal Mode and continues to
 539 race along the global raceline and is unlikely to encounter

540 the opponent until it leads the opponent by an entire lap.
 541 This situation is either likely to happen a long time into the
 542 future (depending on the opponent's comparative
 543 disadvantage, and entirely unlikely if both racecars are the
 544 same) and it may not occur again before the end of the race

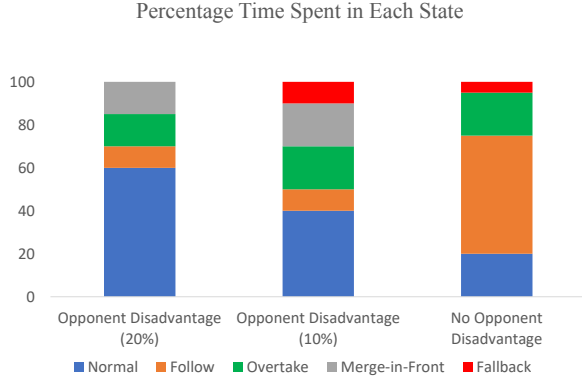


Figure 8: Time spent in each state vs opponent disadvantage

546 Figure 8 shows the amount of time the ego racecar spends
 547 in each state for a lap, averaged for all laps for different
 548 boost energy values and compared to a different opponent
 549 setup. When the ego racecar and opponent have the same
 550 max. rated velocities and the opponent starts in the pole
 551 position, the ego racecar attempts to overtake as seen in
 552 Figure 8[Right], and fails all the time, thus spending most
 553 of the time following the opponent. When the opponent is
 554 slightly disadvantaged in terms of the max. rated velocities
 555 (see Figure 8[Left, Middle]), the ego racecar is more likely
 556 to successfully overtake and merge in front of the opponent
 557 with only a small number of failures. The ego racecar
 558 spends equal amounts of time in both cases to pass the
 559 opponent and then merge in front of the opponent and less
 560 time following the opponent. This demonstrates that, when
 561 considering an equal or slightly disadvantaged opponent, a
 562 leading opponent on the global raceline will continue to
 563 lead the race and the inclusion of the Boost Energy
 564 Management system is necessary to perform the overtake
 565 since the overtake trajectories are often less efficient
 566 compared to the global raceline and the ego racecar needs
 567 the added performance boost to overcome this.

Method	Overtake Attempts	Successful Overtakes	Success Ratio
Reactive Overtake	59	1	0.017
ROS Navigation	26	3	0.115
TEB Planner	14	4	0.286
AutoPass	43	17	0.395

Table 3: Comparison of AutoPass with other methods capable of overtaking. Timed-Elastic Band (TEB) is a plugin to the ROS navigation stack.

568 Table 3 shows the performance of the AutoPass framework
 569 compared to other model free approaches to autonomous
 570 overtaking. We define the success ratio as the number of

571 successful overtakes to the total number of attempted
 572 overtakes. This metric shows (a) the effectiveness of the
 573 method being tested (number of successful overtakes), and
 574 (b) the efficiency of the methods when planning an overtake
 575 maneuver (number of overtake attempts). A purely reactive
 576 system - such as the generic highway lane departure and
 577 pass systems where a vehicle will attempt to take a low
 578 weighted cost passing (overtake) trajectory - produces a
 579 success ratio of 0.017, while the AutoPass system produces
 580 a success ratio of 0.395. The AutoPass framework also
 581 outperforms the standard ROS navigation stack (which has
 582 a 0.115 success ratio), and the more sophisticated TEB
 583 planner [26] (which has a 0.286 success ratio). This
 584 improvement is most likely because the ROS planners
 585 emphasized hard constraints of safety over mission
 586 objective and proved to be extremely risk averse, whereas
 587 AutoPass works with soft constraints for mission objective
 588 while maintaining comparable safety standards.

589 Conclusion

590 In this paper we presented AutoPass - a novel framework
 591 for overtaking in a multi-agent setting. AutoPass uses the
 592 structure of an automaton to break down the complex task of
 593 overtaking into sub-maneuvers that balance overtaking
 594 likelihood and risk with safety of the ego vehicle. We
 595 presented real world implementation of 1/10 scale
 596 autonomous racing using two F1Tenth cars to demonstrate
 597 the effectiveness of AutoPass for the overtaking task. Our
 598 results indicate that the overtake success ratio for the
 599 AutoPass framework is 0.395 or 23 times more likely,
 600 compared to a purely reactive system at 0.017, while
 601 traditional ROS based path planners (depending on the
 602 navigation plugin used) are placed between 0.115 to 0.286.
 603 Our future work on this project is three-fold: first, we are
 604 working on a method to formally verify the AutoPass
 605 automaton to ensure that we can accurately predict when a
 606 successful overtake will be feasible; second, we plan to
 607 incorporate additional racing strategies into the AutoPass
 608 framework (e.g., strategic overtake attempts at certain
 609 sections of a race-track); and finally, we will implement
 610 adversarial characteristics on the opponent to further
 611 improve the AutoPass framework to work under these
 612 conditions.

613 References

1. Global championship of driverless cars.
[url=https://roboreace.com/](https://roboreace.com/), journal=Roborace.
2. Matthew O'Kelly, Varundev Sukhil, Houssam Abbas, Jack Harkins, Chris Kao, Yash Vardhan Pant, Rahul Mangharam, Dipshil Agarwal, Madhur Behl, Paolo Burgio, et al. F1/10: An open-source autonomous cyber-physical platform. *arXiv preprint arXiv:1901.08567*, 2019.
3. Varundev Suresh Babu and Madhur Behl. f1tenths. dev-an open-source ros based f1/10 autonomous

625 racing simulator. In *2020 IEEE 16th International*
 626 *Conference on Automation Science and Engineering*
 627 (*CASE*), pages 1614–1620. IEEE, 2020.

628 4. Albert Boretti. Energy flow of a 2018 fia f1 racing car
 629 and proposed changes to the powertrain rules.
 630 *Nonlinear Engineering*, 9:28–34, 08 2019.

631 5. Nikolce Murgovski and Jonas Sjöberg. Predictive
 632 cruise control with autonomous overtaking. In *2015*
 633 *54th IEEE Conference on Decision and Control*
 634 (*CDC*), pages 644–649. IEEE, 2015.

635 6. Shilp Dixit, Saber Fallah, Umberto Montanaro,
 636 Mehrdad Dianati, Alan Stevens, Francis Mccullough,
 637 and Alexandros Mouzakitis. Trajectory planning and
 638 tracking for autonomous overtaking: State-of-the-art
 639 and future prospects. *Annual Reviews in Control*,
 640 45:76–86, 2018.

641 7. Joshue Perez, Vicente Milanes, Enrique Onieva, Jorge
 642 Godoy, and Javier Alonso. Longitudinal fuzzy control
 643 for autonomous overtaking. In *2011 IEEE*
 644 *International Conference on Mechatronics*, pages
 645 188–193. IEEE, 2011.

646 8. Alexander Buyval, Aidar Gabdulin, Ruslan Mustafin,
 647 and Ilya Shimchik. Deriving overtaking strategy from
 648 nonlinear model predictive control for a race car. In
 649 *2017 IEEE/RSJ International Conference on*
 650 *Intelligent Robots and Systems (IROS)*, pages
 651 2623–2628. IEEE, 2017.

652 9. A. Buyval, A. Gabdulin, R. Mustafin, and I. Shimchik.
 653 Deriving overtaking strategy from nonlinear model
 654 predictive control for a race car. In *2017 IEEE/RSJ*
 655 *International Conference on Intelligent Robots and*
 656 *Systems (IROS)*, pages 2623–2628, 2017.

657 10. H. Huang and T. Wang. Learning overtaking and
 658 blocking skills in simulated car racing. In *2015 IEEE*
 659 *Conference on Computational Intelligence and Games*
 660 (*CIG*), pages 439–445, 2015.

661 11. D. Loiacono, A. Prete, P. L. Lanzi, and L. Cardamone.
 662 Learning to overtake in torcs using simple
 663 reinforcement learning. In *IEEE Congress on*
 664 *Evolutionary Computation*, pages 1–8, 2010.

665 12. Alexander Liniger and John Lygeros. A
 666 non-cooperative game approach to autonomous racing,
 667 2019.

668 13. Tim Stahl, Alexander Wischnewski, Johannes Betz,
 669 and Markus Lienkamp. Multilayer graph-based
 670 trajectory planning for race vehicles in dynamic
 671 scenarios. *2019 IEEE Intelligent Transportation*
 672 *Systems Conference (ITSC)*, Oct 2019.

673 14. Trent Weiss and Madhur Behl. Deepracing: a
 674 framework for autonomous racing. In *2020 Design,*
 675 *Automation & Test in Europe Conference & Exhibition*
 676 (*DATE*), pages 1163–1168. IEEE, 2020.

677 15. Zheng Zhang, Peifeng Gao, Zilong He, Hongbin Chen,
 678 and Jianfeng Wang. Autonomous driving system
 679 design for formula racing. In *Journal of Physics: Conference Series*, volume 1651, page 012125. IOP
 680 Publishing, 2020.

682 16. Alexander Liniger, Alexander Domahidi, and Manfred
 683 Morari. Optimization-based autonomous racing of 1:
 684 43 scale rc cars. *Optimal Control Applications and*
 685 *Methods*, 36(5):628–647, 2015.

686 17. B. Houska, H.J. Ferreau, and M. Diehl. ACADO
 687 Toolkit – An Open Source Framework for Automatic
 688 Control and Dynamic Optimization. *Optimal Control*
 689 *Applications and Methods*, 32(3):298–312, 2011.

690 18. Keith R Pullen. The status and future of flywheel
 691 energy storage. *Joule*, 3(6):1394–1399, 2019.

692 19. Wikipedia. Push-to-pass, 2020. [Online; accessed
 693 15-Dec-2020].

694 20. D. Choi. Development of open-source motor
 695 controller framework for robotic applications. *IEEE*
 696 *Access*, 8:14134–14145, 2020.

697 21. Corey Walsh and Sertac Karaman. Cddt: Fast
 698 approximate 2d ray casting for accelerated
 699 localization. *abs/1705.01167*, 2017.

700 22. Zheng Zhang, Peifeng Gao, Zilong He, Hongbin Chen,
 701 and Jianfeng Wang. Autonomous driving system
 702 design for formula racing. In *Journal of Physics: Conference Series*, volume 1651, page 012125. IOP
 703 Publishing, 2020.

705 23. Robin Verschueren, Stijn De Bruyne, Mario Zanon,
 706 Janick V Frasch, and Moritz Diehl. Towards
 707 time-optimal race car driving using nonlinear mpc in
 708 real-time. In *53rd IEEE conference on decision and*
 709 *control*, pages 2505–2510. IEEE, 2014.

710 24. Z. Lu, B. Shyrokau, B. Boulkroune, S. van Aalst, and
 711 R. Happee. Performance benchmark of state-of-the-art
 712 lateral path-following controllers. In *2018 IEEE 15th*
 713 *International Workshop on Advanced Motion Control*
 714 (*AMC*), pages 541–546, 2018.

715 25. Nishant Chowdhri, Laura Ferranti, Felipe Santafé
 716 Iribarren, and Barys Shyrokau. Integrated nonlinear
 717 model predictive control for automated driving.
 718 *Control Engineering Practice*, 106:104654, 2021.

719 26. Christoph Rösmann, Frank Hoffmann, and Torsten
 720 Bertram. Integrated online trajectory planning and
 721 optimization in distinctive topologies. *Robotics and*
 722 *Autonomous Systems*, 88:142–153, 2017.